

RESEARCH ARTICLE

Nup153 and Nup50 promote recruitment of 53BP1 to DNA repair foci by antagonizing BRCA1-dependent events

Douglas R. Mackay^{1,*}, Amanda C. Howa¹, Theresa L. Werner² and Katharine S. Ullman^{1,*}

ABSTRACT

DNA double-strand breaks are typically repaired through either the high-fidelity process of homologous recombination (HR), in which BRCA1 plays a key role, or the more error-prone process of non-homologous end joining (NHEJ), which relies on 53BP1. The balance between NHEJ and HR depends, in part, on whether 53BP1 predominates in binding to damage sites, where it protects the DNA ends from resection. The nucleoporin Nup153 has been implicated in the DNA damage response, attributed to a role in promoting nuclear import of 53BP1. Here, we define a distinct requirement for Nup153 in 53BP1 intranuclear targeting to damage foci and report that Nup153 likely facilitates the role of another nucleoporin, Nup50, in 53BP1 targeting. The requirement for Nup153 and Nup50 in promoting 53BP1 recruitment to damage foci induced by either etoposide or olaparib is abrogated in cells deficient for BRCA1 or its partner BARD1, but not in cells deficient for BRCA2. Together, our results further highlight the antagonistic relationship between 53BP1 and BRCA1, and place Nup153 and Nup50 in a molecular pathway that regulates 53BP1 function by counteracting BRCA1-mediated events.

KEY WORDS: Nup153, Nup50, Nuclear pore complex, 53BP1, BRCA1, DNA damage

INTRODUCTION

When genomic DNA is damaged, a protective response rapidly ensues involving events ranging from local changes in chromatin and intricate mechanisms of DNA repair to concomitant cell cycle arrest (Daley and Sung, 2014; Smith-Roe et al., 2015). The DNA damage response is remarkably extensive, but central events are the deposition and hallmark modification of the variant histone H2AX [phosphorylated at serine 139 (Rogakou et al., 1998) referred to as γ -H2AX] and the subsequent recruitment of repair factors, such as MDC1, RNF8 and RNF168 to nuclear foci where DNA repair takes place. Downstream events then dictate which DNA repair mechanisms are implemented. For instance, recruitment of 53BP1 protects the damaged DNA end from undergoing resection, which in turn prevents homologous recombination (HR) repair and, instead, promotes non-homologous end-joining (NHEJ) (Bunting et al., 2010; Cao et al., 2009; Kakarougkas et al., 2013; Zimmermann and de Lange, 2014). Conversely, BRCA1 (Chapman et al., 2012) and factors it recruits,

such as UHRF1 (Zhang et al., 2016) and CtIP (Escribano-Diaz et al., 2013), counter 53BP1-mediated events and lead to HR repair.

Tumor cells often bear defects in the DNA damage response or in cell cycle checkpoints required to provide time to cope with the consequences of DNA damage. These defects can underlie a level of genomic instability that enables tumorigenesis. Exploiting these acquired deficiencies has, in turn, long been a cornerstone of therapy in oncology. Inhibition of poly(ADP-ribose) polymerase (PARP) is an elegant example of such a strategy (Bryant et al., 2005; Farmer et al., 2005). These inhibitors work synergistically with defects in the HR repair pathway, with cells bearing HR defects 100–1000-fold more sensitive to such treatment (Farmer et al., 2005). The PARP inhibitor (PARPi) olaparib is now, under some circumstances, FDA approved as monotherapy for ovarian cancer patients bearing germline mutations in *BRCA1* or *BRCA2*, which result in defective HR repair (Sandhu et al., 2010). Clinical trials are also currently conducted to test PARP inhibitors in the treatment of breast, pancreatic, prostate, gastric and brain tumors, and show signs of success (Ricks et al., 2015). Yet, even in cases where their efficacy seems assured (e.g. tumors with mutations in *BRCA1* or *BRCA2*), PARP inhibitors do not always work in the clinic as predicted (Liu et al., 2014; Lord and Ashworth, 2013). Numerous factors can influence the DNA damage response and, in turn, contribute to sensitivity to PARP inhibition. With a more complete mechanistic understanding of DNA damage response pathways, we will ultimately be able to apply a more sophisticated algorithm to predict tumor response and to achieve better clinical outcomes by tailoring treatment appropriately.

In the case of PARP inhibition, NHEJ DNA repair has emerged as a molecular pathway critical to tumor response (Patel et al., 2011). When the combination of PARP inhibition and tumor defects in HR repair result in unprotected DNA ends, the NHEJ pathway promotes end fusion. It is thought that the overuse of this repair pathway ultimately results in a level of chromosome fusions that are detrimental to the cell. Indeed, in pre-clinical mouse models of breast cancer, the loss of NHEJ factors, such as 53BP1 (Jaspers et al., 2013) or the downstream effector REV7 (Xu et al., 2015), results in resistance to PARP inhibition. The importance of the NHEJ pathway has focused attention on 53BP1 as a potential biomarker of PARPi response (Oplustilova et al., 2012; Yang et al., 2015). Clearly, though, 53BP1 not only needs to be present, but must also function appropriately for the execution of NHEJ. Thus, factors that influence 53BP1 activity are equally important to scrutinize in this context, as their disruption could lead to PARPi resistance.

The nuclear pore protein Nup153 is reported to be required for the recruitment of 53BP1 to DNA damage foci and for maintaining the balance between NHEJ and HR repair (Lemaitre et al., 2012; Moudry et al., 2012). In particular, these reports suggest a selective reliance on Nup153 for the import of 53BP1 into the nucleus. Such a role for Nup153 indicates that levels of this protein may influence

¹Department of Oncological Sciences, Huntsman Cancer Institute, University of Utah, Salt Lake City, UT 84112, USA. ²Department of Medicine, Division of Oncology, Huntsman Cancer Institute, University of Utah, Salt Lake City, UT 84112, USA.

*Authors for correspondence (Douglas.Mackay@hci.utah.edu; Katharine.Ullman@hci.utah.edu)

DOI: 10.1242/jcs.203513

whether 53BP1 functions correctly and, in turn, whether a tumor will be sensitive to PARP inhibition, as noted by Moudry and colleagues (Moudry et al., 2012). In the course of probing the role of Nup153 and evaluating its potential as a biomarker for PARPi sensitivity, we have made several surprising observations. We demonstrate here that Nup153 plays two roles in 53BP1 function, influencing both nucleocytoplasmic distribution and an additional separable step in intranuclear targeting of 53BP1. We find that a second nuclear pore protein, Nup50, is also critical for targeting 53BP1 to DNA damage foci, but appears dispensable for its nuclear import. Interaction with Nup50 is required for the role of Nup153 in intranuclear 53BP1 targeting, and elevated levels of Nup50 can compensate for reduced levels of Nup153. Yet, despite the clear contributions of these nucleoporins to the function of 53BP1, we observed that low levels of Nup153 or Nup50 do not influence the sensitivity to PARPi following BRCA1 depletion. Further experiments revealed that BRCA1 deficiency promotes the recruitment of 53BP1 to nuclear foci and overrides a requirement for Nup153 or Nup50 function. Similar results were observed upon depletion of the cofactor BARD1, suggesting that the function of BRCA1 in this context requires its ubiquitin ligase activity. This cross-talk is selective as deficiency in BRCA2, another component of the HR repair pathway, did not relieve a requirement for Nup153 or Nup50. These results lend important new insight into the circuitry of the DNA damage response and underscore the need to fully understand these pathways in order to capitalize on this knowledge in the clinic.

RESULTS

Nup153 and Nup50 are required for focal recruitment of 53BP1 in response to DNA damage, and function at two separable steps in this process

The nuclear pore complex (NPC) is an ornate macromolecular complex, with eightfold symmetrical subunits that form a central channel flanked by unique structural features on the cytoplasmic and nuclear faces. On the nuclear face, eight filaments extend from the ring of the pore and attach to a distal, smaller ring, creating a feature referred to as the nuclear pore basket (Knockenbauer and Schwartz, 2016). The pore protein Nup153 is a key component of this NPC sub-structure (Hase and Cordes, 2003). A question that arises from the newly appreciated role for Nup153 in 53BP1 function is whether this is a role of the NPC nuclear basket as a unit or a specific role of Nup153. To address this question, we compared the effects of depleting Nup153 versus other components of this NPC sub-structure, i.e. Nup50 and Tpr. Small interfering RNA (siRNA) oligonucleotides specific to each nucleoporin were used to deplete these NPC basket components from U2OS cells. Western blot analysis confirmed that each protein was reduced without disrupting levels of the other basket components (Fig. 1C; Fig. S1A). Consistent with previous results, cells depleted of Nup153 displayed elevated levels of 53BP1 within the cytoplasm (Fig. 1A,B). We then treated cells with etoposide, which inhibits topoisomerase II and generates DNA double-strand breaks. Following induction of DNA damage in this manner, we observed that both Nup153-depleted and Nup50-depleted cells displayed markedly reduced numbers of 53BP1-positive damage foci compared to control-treated cells (from an average of >20 foci per cell to the range of five foci per cell in three independent experiments, Fig. 1A,B,D; Fig. S1B,C). This occurred despite the fact that total cellular levels of 53BP1 (Fig. 1C) – as well as other upstream aspects of the DNA damage response, namely MDC1 recruitment and H2AX recruitment and modification – were

unaffected (Fig. 1A,B). In contrast, depletion of Tpr had little effect on 53BP1 targeting (Fig. 1), indicating that intranuclear targeting of 53BP1 to damage foci depends selectively on Nup153 and Nup50. These observations were confirmed with independent siRNA oligonucleotides (Fig. 1D; Fig. S1).

53BP1 promotes NHEJ predominantly during G1 phase of the cell cycle by suppressing BRCA1 accumulation in a RIF1-dependent manner (Escribano-Diaz et al., 2013). To determine whether depletion of Nup153 or Nup50 results in alterations in cell cycle distribution that might account for fewer cells displaying 53BP1 foci, we quantified the percentage of the cell population that was positive for cyclin A after treatment with the corresponding siRNA oligonucleotides and induction of DNA damage with etoposide. The distribution of cyclin A-positive cells (S/G2 phase) remained relatively unchanged under these conditions, regardless of the levels of Nup153 or Nup50 (Fig. S1D), indicating that the reduction in 53BP1 targeting described here is not a secondary effect of an altered cell cycle distribution. With 53BP1 foci formation most robust in G1 phase cells, we further found that impaired focal targeting of 53BP1 in the absence of Nup153 or Nup50 is more pronounced in G1 phase cells than in S/G2 phase cells (Fig. 1E).

As upstream events in DNA damage response appeared intact, we next evaluated localization of the downstream factor RIF1 (Di Virgilio et al., 2013; Zimmermann et al., 2013) under the same experimental conditions. Consistent with its reported dependence on 53BP1 for targeting to sites of DNA damage, RIF1 foci formation was markedly impaired upon depletion of either Nup153 or Nup50 (Fig. 1F). Yet, the observed disruption in recruitment of 53BP1 and RIF1, factors important for repair of DNA lesions through the NHEJ pathway, was not accompanied by an increase in the number of G1 phase cells displaying Rad51 foci (Fig. 1G), indicating that the HR pathway is not aberrantly activated in G1 phase cells in the absence of Nup153 or Nup50.

While depletion of Nup153 or Nup50 clearly led to a significant reduction in the number of 53BP1 foci in cells, we observed that, following either Nup153 or Nup50 depletion, ~20–40% of the cell population still displayed some 53BP1 foci formation (Fig. S1E). These foci, however, were consistently smaller and measurably less fluorescently intense when compared to cells treated with control siRNA (Fig. 2). Reduced 53BP1 recruitment was not due to a reduction in the total amount of 53BP1 within cells, which remained relatively unchanged (Fig. 1C). Quantitative examination of individual foci revealed that the intensity of MDC1 was not affected (Fig. 2), further underscoring that Nup153 and Nup50 have a specific role in the intranuclear targeting of 53BP1 to DNA double-strand break repair foci. In *Saccharomyces cerevisiae*, DNA double-strand breaks localize to a limited number of sites at the nuclear periphery through interaction with the NPC and other nuclear envelope proteins (Horigome et al., 2016; Nagai et al., 2008; Oza et al., 2009). Similar biased localization of double-strand breaks in mammalian cells has not been reported (reviewed in Kalousi and Soutoglou, 2016). Under the conditions used throughout this study, we also observed an apparently random distribution of damage foci (with and without 53BP1) regardless of the levels of Nup153 or Nup50 (Fig. 1A,B and Fig. 2A), indicating that the defects in 53BP1 targeting reported here do not take place selectively at the NPC or nuclear periphery.

Although depletion of Nup153 leads to alteration of the nuclear pore basket, NPCs are still prevalent (Duheron et al., 2014; Hase and Cordes, 2003; Jacinto et al., 2015; Mackay et al., 2009, 2010). Under the conditions of depletion used here, the NPC basket defect

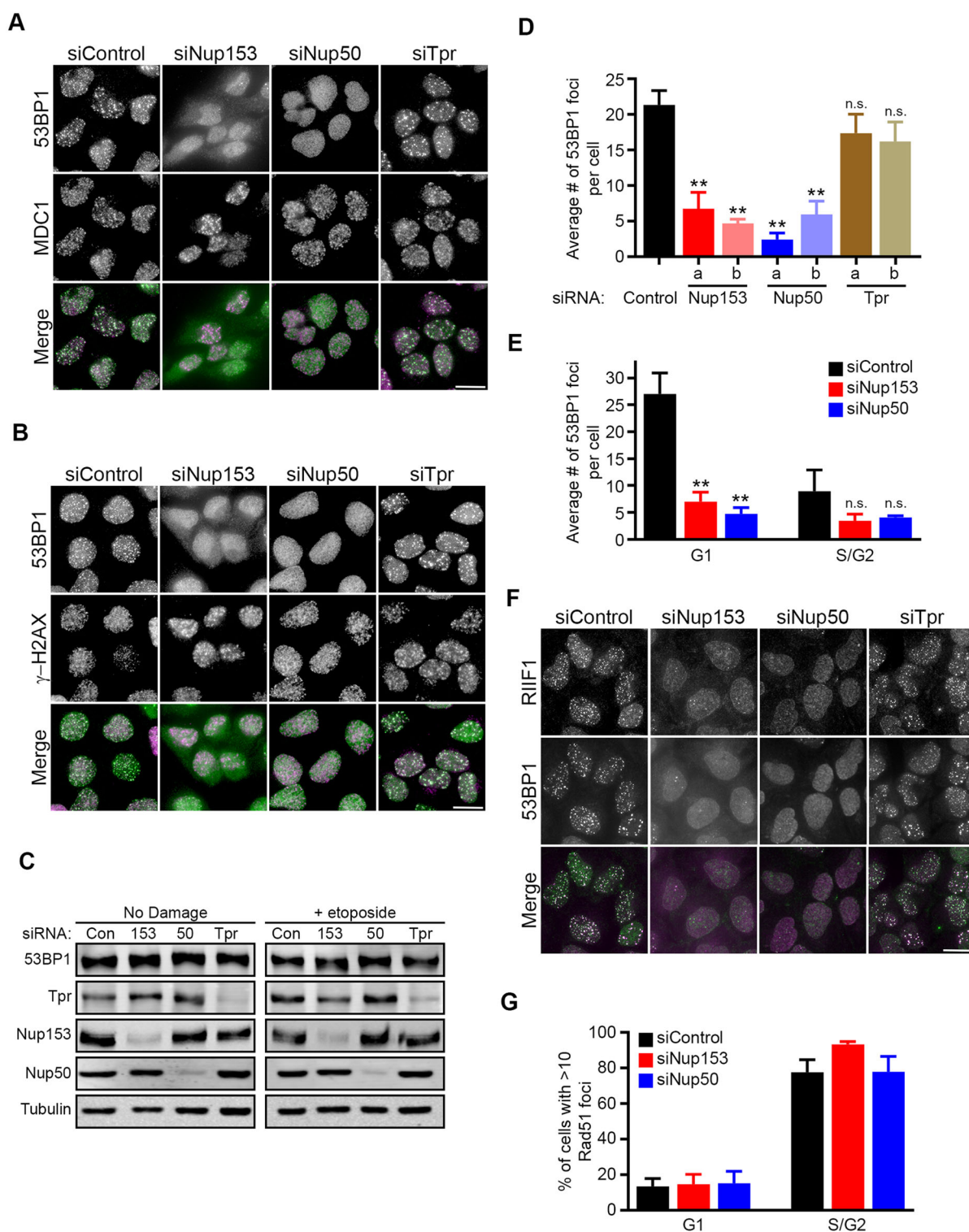


Fig. 1. 53BP1 foci formation depends on both Nup153 and Nup50, but not a third NPC basket protein, Tpr. (A, B) U2OS cells were transfected with either control or gene-specific siRNAs as indicated. 48 h later, cells were treated with 20 μ M etoposide for 30 min, followed by a 90 min recovery period in fresh medium, and analyzed for the formation of nuclear 53BP1 foci (green). DNA damage foci were detected by using antibodies against MDC1 (A; magenta) or γ -H2AX (B; magenta). Results from experiments using the 'a' siRNA oligonucleotides are illustrated in A–C and E–G, while results using the independent 'b' siRNA oligonucleotides are illustrated in Fig. S1. (C) Western blot analysis confirmed knockdown of the indicated proteins in the absence or presence of DNA damage. Note that total cellular levels of 53BP1 are not affected after depletion of Nup153 or Nup50. (D) Quantification of the average number of 53BP1 foci per cell. Error bars throughout this figure represent the mean and standard deviation from three independent experiments where >100 cells were scored. ** P <0.001; n.s., not significant; compared to control siRNA (Student's t -test). (E) Quantification of 53BP1 foci in cyclin A-negative (G1) and cyclin A-positive (S/G2) cells upon induction of DNA damage after treatment with the indicated siRNAs. Error bars and statistical analysis are the same as in D. (F) Cells were treated with the indicated siRNAs, incubated for 30 min in 20 μ M etoposide, and analyzed for nuclear foci containing RIF1 (green) or 53BP1 (magenta). (G) Quantification of cyclin A-negative (G1) and cyclin A-positive (S/G2) cells with >10 Rad51 foci in percent. All scale bars: 20 μ m.

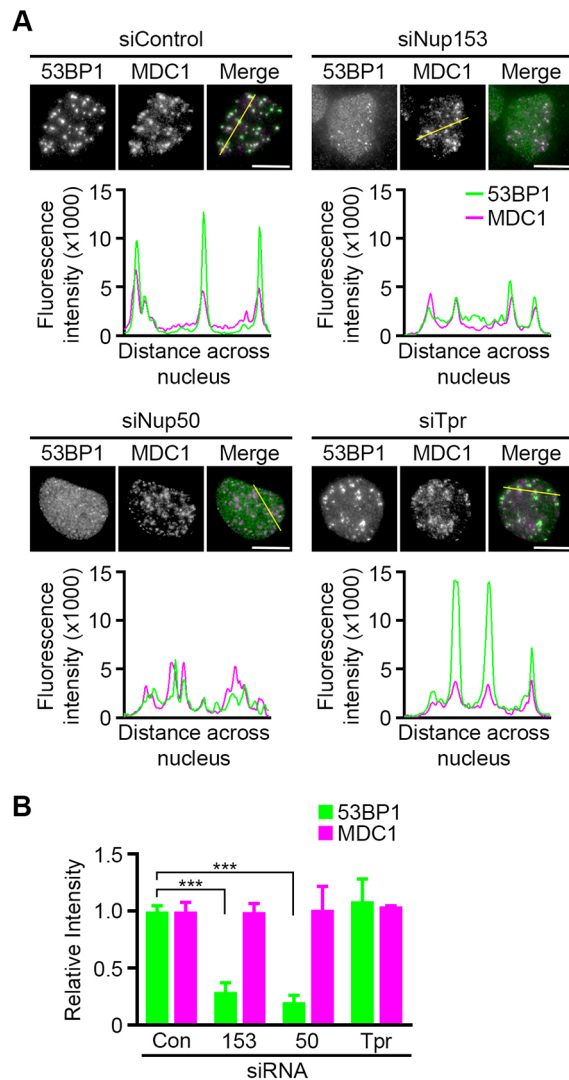


Fig. 2. In addition to being fewer in number, 53BP1 foci are smaller and show less intense fluorescence staining when Nup153 and Nup50 are depleted. (A) Fluorescence intensity of nuclear 53BP1 foci from single cells as described in Fig. 1A was quantified along a line drawn through the nucleus. Distinct peaks in graphs indicate intensity measurements of 53BP1 (green) and MDC1 (magenta) at individual DNA damage foci. Scale bars: 10 μ m. (B) Quantification of peak fluorescence intensity relative to control siRNA. A single line was drawn in ten cells per experiment, and peak MDC1 intensity was used to determine damage foci. Error bars represent the mean and standard deviation from three independent experiments. *** $P < 0.0001$ (Student's *t*-test).

is more prominent in recently divided cells (Mackay et al., 2010). At a functional level, both bulk mRNA export as well as import mediated by a canonical nuclear localization sequence (NLS) have been found to remain robust when Nup153 levels are reduced. This implies that Nup153 makes a specialized contribution to 53BP1 import. Further, the contributions Nup153 makes to the import and intranuclear targeting of 53BP1 could be separable. To test this, we generated cell lines stably expressing either GFP-53BP1 or GFP-53BP1 fused to a potent NLS (GFP-53BP1-NLS). We found that, while GFP-53BP1 – like endogenous 53BP1 – was partially mislocalized to the cytoplasm following Nup153 depletion, GFP-53BP1-NLS was present only within the nucleus, indicating that addition of a strong NLS overcame the dependence of 53BP1 on Nup153 for efficient import (Fig. 3A,B). Nonetheless, after treatment with etoposide, 53BP1 foci formation was still

disrupted, whether tracking either GFP-53BP1 or GFP-53BP1-NLS in cells depleted of Nup153 or Nup50 (Fig. 3). This was not due to the fact that these are fusion proteins as they responded normally to DNA damage when cells were treated with a control siRNA oligonucleotide. Together, these results indicate that Nup153 has two different roles: one which promotes the nuclear import of 53BP1 and another that is critical for the intranuclear targeting of 53BP1. The uncoupling of these roles is further supported by the observation that Nup50 depletion has a robust effect on 53BP1 foci formation without altering the ability of 53BP1 to accumulate in the nucleus (Fig. 1A,B).

Nup153 has also been implicated in efficient export of microRNAs (miRNAs) in response to DNA damage (Wan et al., 2013). This role is unlikely to influence the immediate response to DNA damage since not just export, but also miRNA-mediated alterations in translation and mRNA stability, must occur for its functional manifestation. Given these kinetic considerations, we wanted to determine whether or not Nup153 is required for initial 53BP1 targeting. To do so, we assessed very early time points following induction of DNA damage. Looking at cells immediately after etoposide exposure, we found that the number 53BP1 foci in cells was markedly decreased as early as 15 min after DNA damage when either Nup153 or Nup50 was depleted (Fig. 4A,B). This early defect was independent of alterations in nuclear import, as GFP-53BP1-NLS was similarly affected (Fig. 4C,D). Thus, there is a requirement for Nup153 and Nup50 in 53BP1 targeting at very early stages of the DNA damage response, which is likely distinct from the role of Nup153 in DNA damage-induced miRNA export.

Despite being components of an architectural substructure of the NPC, Nup153 and Nup50 are known to reside transiently at this site, in dynamic exchange with a nucleoplasmic population (Buchwalter et al., 2014; Daigle et al., 2001; Griffis et al., 2004). The existence of nucleoplasmic populations of these nuclear pore proteins raises the question of whether they might themselves localize to intranuclear sites where damaged DNA is repaired. This has been examined previously for Nup153 and was not found to be the case (Lemaître et al., 2012). Since Nup153 and Nup50 have somewhat different dynamics at the NPC and other functional distinctions (Dultz et al., 2008; Jacinto et al., 2015; Rabut et al., 2004), we investigated whether Nup50 shifted its steady-state localization to sites of damage. Tracking either endogenous or GFP-fusion proteins, we found that, like Nup153, Nup50 does not appear at these sites, even at very early stages of the DNA damage response (Fig. S2). Together, these results suggest that Nup153 and Nup50 play an important role in promoting the recruitment of 53BP1 without accumulating at these same sites of DNA damage.

To verify that the observed phenotype with respect to intranuclear targeting of 53BP1 is specific to depletion of Nup153 and Nup50, we generated U2OS cell lines that stably express siRNA-resistant GFP fusions of either Nup153 or Nup50, and assessed whether expression of these proteins can rescue the 53BP1-targeting defect. Expression of Nup153-GFP or Nup50-GFP restored targeting of 53BP1 to DNA damage foci following treatment with Nup153-specific or Nup50-specific siRNA oligonucleotides, respectively (Fig. 5). Surprisingly, Nup50-GFP expression was also able to rescue recruitment of 53BP1 after Nup153 depletion (Fig. 5B,D). By contrast, Nup153 overexpression did not mitigate 53BP1 recruitment defects in Nup50-depleted cells (Fig. 5A,C). This pattern of cross-rescue suggests that Nup153 facilitates Nup50 function in DNA damage response. We next capitalized on this rescue strategy in order to test whether Nup153 function requires its ability to bind Nup50. Our lab had previously identified a region of

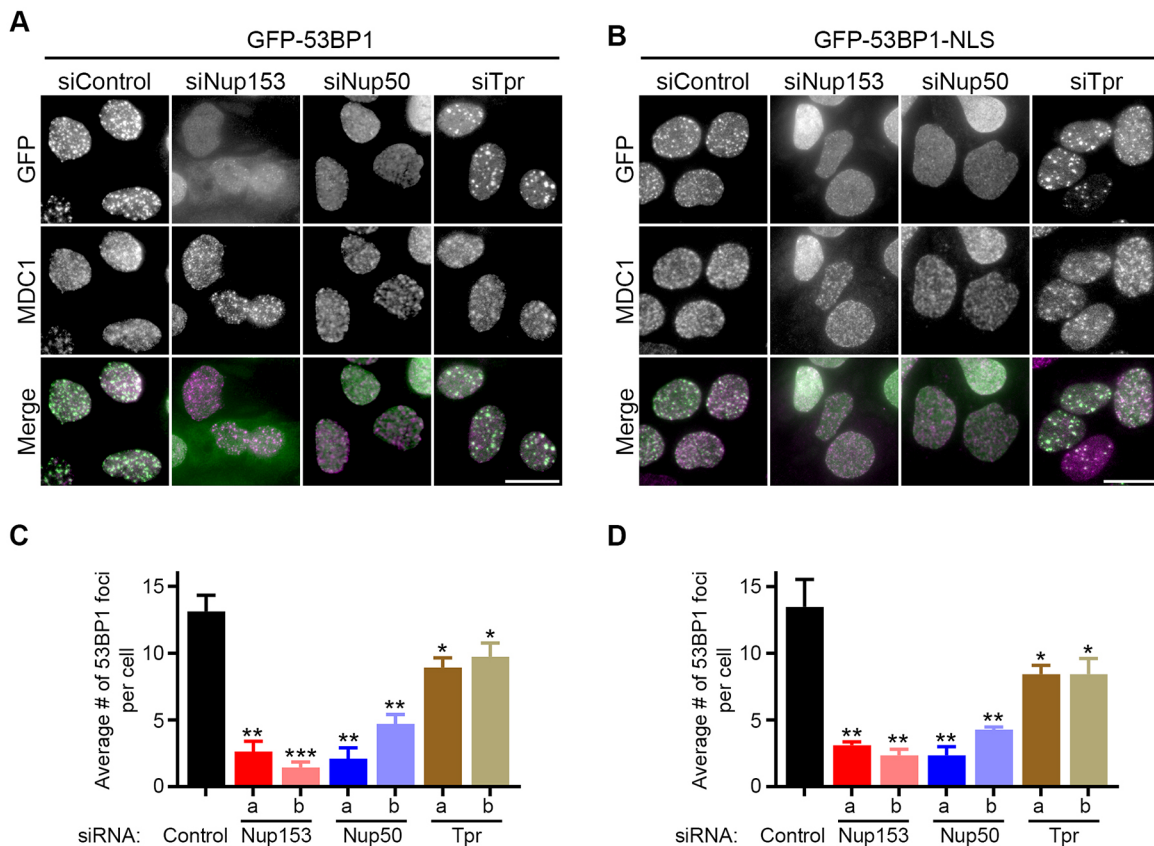


Fig. 3. Nup153 contributes to both nuclear import and intranuclear targeting of 53BP1. (A,B) U2OS cells stably expressing GFP-53BP1 (A) or GFP-53BP1-NLS (B) were transfected with the indicated siRNA oligonucleotides and treated with etoposide as described for Fig. 1A. DNA damage foci were detected by using an antibody against MDC1 and recruitment of GFP-53BP1 or GFP-53BP1-NLS was assessed by using an antibody directed against GFP (green). Scale bars: 20 μ m. (C,D) Quantification of the number of GFP-53BP1 or GFP-53BP1-NLS foci per cell (detected by GFP) upon induction of DNA damage after treatment with the indicated siRNA oligonucleotides. Error bars represent the mean and standard deviation from three independent experiments where >100 cells were scored. *** P <0.0001, ** P <0.001, * P <0.02; compared to control siRNA (Student's t -test).

Nup153 (amino acids 401–609) that is required for interaction with Nup50 (Makise et al., 2012). Here, we generated a range of U2OS cell lines stably expressing a series of Nup153 variants with progressively smaller deletions within the Nup50-binding domain (Fig. 6A). These fusion proteins, which display the characteristic localization of full-length Nup153-GFP (Figs. 5A and 6C), were then captured from cell lysates by using a GFP-trap assay. Probing for recovery of endogenous Nup50 in association with these variants of Nup153 revealed that the internal deletions all disrupted the ability of Nup153 to interact with Nup50. Even the shortest deletion, which removed 59 amino acids, is significantly – albeit not completely – compromised for Nup50 binding (Fig. 6B). Moreover, stable expression of these mutants did not rescue the defect in 53BP1 focal targeting seen following the depletion of endogenous Nup153 (Fig. 6C,D). Thus, the function of Nup153 in 53BP1 intranuclear targeting requires interaction with Nup50.

Low levels of Nup153 or Nup50 do not interfere with PARPi sensitivity in BRCA1-deficient cells

PARP inhibitors are exciting options as a selective pharmacological treatment of BRCA1- or BRCA2-deficient tumors (Benafif and Hall, 2015). Response to PARP inhibition was found to be dependent on 53BP1 (Jaspers et al., 2013), which is thought to promote the error-prone process of NHEJ at sites left vulnerable from the combination of PARPi-induced DNA damage and HR repair defects. The over-use of NHEJ under these circumstances

creates chromosome fusions and aberrancies that, eventually, lead to cell death. Indeed, in a pre-clinical model of BRCA1-associated breast cancer, tumors develop resistance to PARPi treatment through loss of 53BP1 (Jaspers et al., 2013). Since our data indicate that Nup153 and Nup50 are required for intranuclear targeting of 53BP1, and because Nup153 depletion has been reported to result in increased levels of HR repair (Lemaitre et al., 2012), we predicted that low levels of these nucleoporins would also result in PARPi resistance in cells deficient for BRCA1. To test this prediction, we treated cells with either control, Nup153 or Nup50 siRNA and then, 24 h later, subjected cells to treatment with either control or BRCA1 siRNA (Fig. 7A). On the third day, cells were plated in 96-well assay plates and incubated with increasing concentrations of the PARPi olaparib. Cell viability was determined 5 days later. As expected, BRCA1-deficient cells demonstrated a marked sensitivity to olaparib treatment (IC_{50} =37.2 nM) compared with control cells (IC_{50} =6.8 μ M), which was largely reversed when 53BP1 was co-depleted (IC_{50} =1.7 μ M; Fig. 7C). Interestingly, contrary to our prediction, depletion of neither Nup153 nor Nup50 counteracted PARPi sensitivity in BRCA1-deficient cells (Fig. 7D, E), despite confirmation that protein levels corresponded to the respective siRNA treatments (Fig. 7B).

To further understand the connections between BRCA1, 53BP1, Nup153 and Nup50, and to explore why low levels of Nup153 or Nup50 did not result in PARPi resistance, we examined the response of 53BP1 to DNA damage more directly in control and BRCA1-

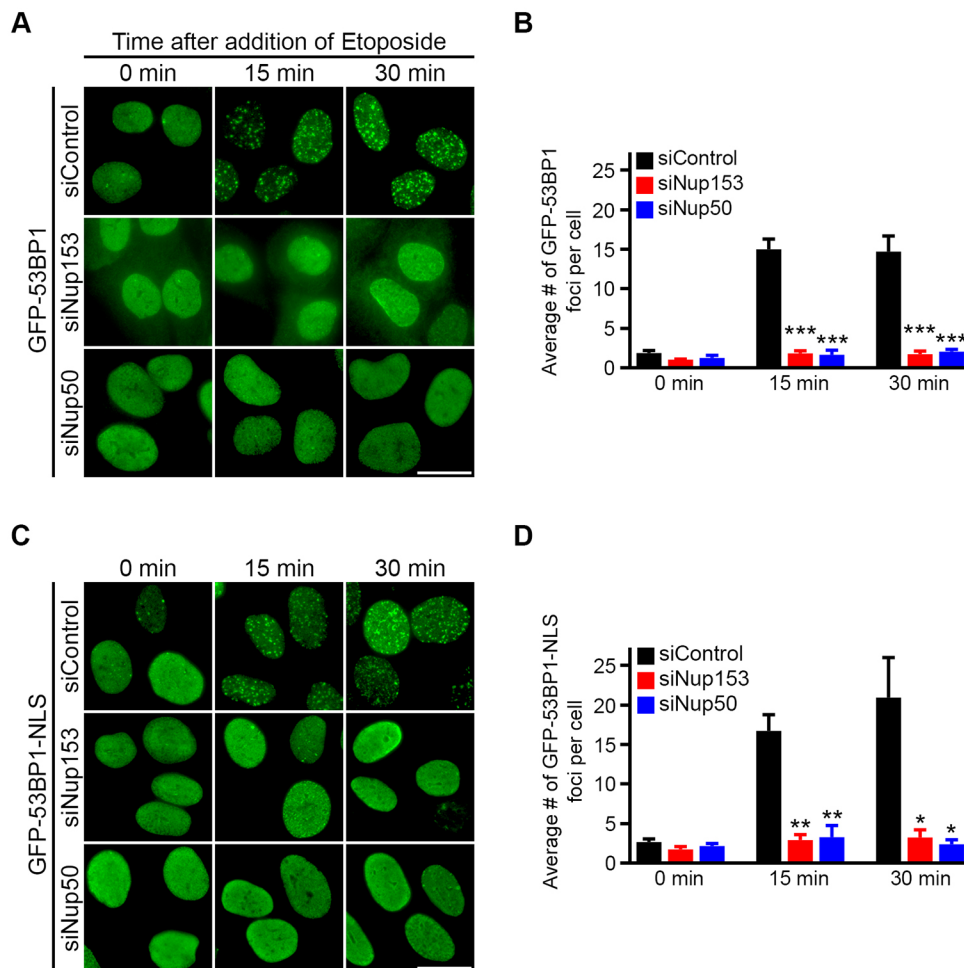


Fig. 4. Both Nup153 and Nup50 are required at very early stages of the DNA damage response. (A,C) U2OS cells expressing GFP-53BP1 (A) or GFP-53BP1-NLS (C) depleted of the indicated proteins were treated with 20 μ M etoposide and cells harvested for analysis every 5 min for 30 min. Shown here are examples from 15 min and 30 min after addition of etoposide. Scale bar: 20 μ m. (B,D) Quantification of the number of GFP-53BP1 or GFP-53BP1-NLS foci per cell (detected by GFP) upon induction of DNA damage after treatment with the indicated siRNA oligonucleotides. Error bars represent the mean and standard deviation from three independent experiments where >100 cells were scored. * P <0.005, ** P <0.001, *** P <0.0001; compared to control siRNA at each time point (Student's t -test).

depleted cells that had been first treated with Nup153 or Nup50 siRNA. In BRCA1-deficient cells, we observed an elevated number of nuclear 53BP1 foci, even without induction of DNA damage following treatment with PARPi (Fig. 8A,B). Following olaparib treatment, BRCA1-deficient cells also responded with higher numbers of 53BP1 foci (Fig. 8C,D). Depletion of Nup153 concurrently with BRCA1 resulted in some reduction of 53BP1 foci formation but, overall, this response remained robust, reaching the levels seen in cells that had been exposed only to control siRNA (~25 foci per cell). Depletion of Nup50 in the setting of BRCA1 deficiency did little to the efficiency of 53BP1 foci formation following olaparib exposure. These results indicate that intranuclear 53BP1 targeting can occur independently of Nup153 and Nup50 and in the absence of BRCA1. This 53BP1 response status is consistent with the BRCA1-deficient cells being refractory to changes in Nup153 and Nup50 levels in PARPi sensitivity assays (Fig. 7D,E), where 53BP1 is thought to generate toxic consequences of PARP inhibition (Jaspers et al., 2013). Similarly, BRCA1 depletion conferred independence from Nup153 and Nup50 with respect to 53BP1 recruitment to foci following etoposide treatment (Fig. 8E,F). Notably, these conditions do not simply reveal a general enhancement of 53BP1 focal intensity when BRCA1 is reduced, because we did not detect a difference in the fluorescence intensity of foci in the absence and presence of BRCA1 unless Nup153 or Nup50 was also depleted (Fig. S3C).

We next asked whether Nup153 and Nup50 have a specific connection to BRCA1 function or whether the role of these

nucleoporins in the DNA damage response is connected to a more general requirement for functional HR repair. To this end, we examined how levels of Nup153 and Nup50 affect DNA damage response when cells are deficient in BRCA2 activity. BRCA2, named for its discovery as the second gene connected to genetic predisposition to breast cancer, is a distinct protein which has a role downstream of BRCA1 in the HR repair pathway (Moynahan et al., 2001; Tutt et al., 2001). Cells deficient in BRCA2 are similar to BRCA1-deficient cells in their sensitivity to inhibition of PARP activity (Farmer et al., 2005) (Fig. S3). However, when tested in the visual assay for 53BP1 foci formation, BRCA2-deficient cells differed from BRCA1-deficient cells in that they depended on Nup153 and Nup50 activity in order to execute the response of 53BP1 foci formation following exposure to either PARPi or etoposide (Fig. 8C-F). These results underscore that BRCA1 status, but not that of HR repair in general, dictates sensitivity to decreased levels of Nup153 or Nup50. Supporting this conclusion, treatment of cells with mirin, a small-molecule inhibitor of the exonuclease activity of the Mre11–Rad50–Nbs1 (MRN1) complex, which plays a role in DNA resection during HR repair (Dupré et al., 2008), was not sufficient to restore 53BP1 recruitment in cells depleted of Nup153 or Nup50 (Fig. S3D).

BRCA1 works in concert with its cofactor BRCA1-associated RING domain protein 1 (BARD1) – which is required for the E3 ubiquitin ligase activity of BRCA1 – to facilitate displacement of 53BP1 from damaged chromatin (Densham et al., 2016; Densham and Morris, 2017). We tested whether depletion of BARD1 and the consequent impairment of BRCA1 ubiquitin ligase activity, is

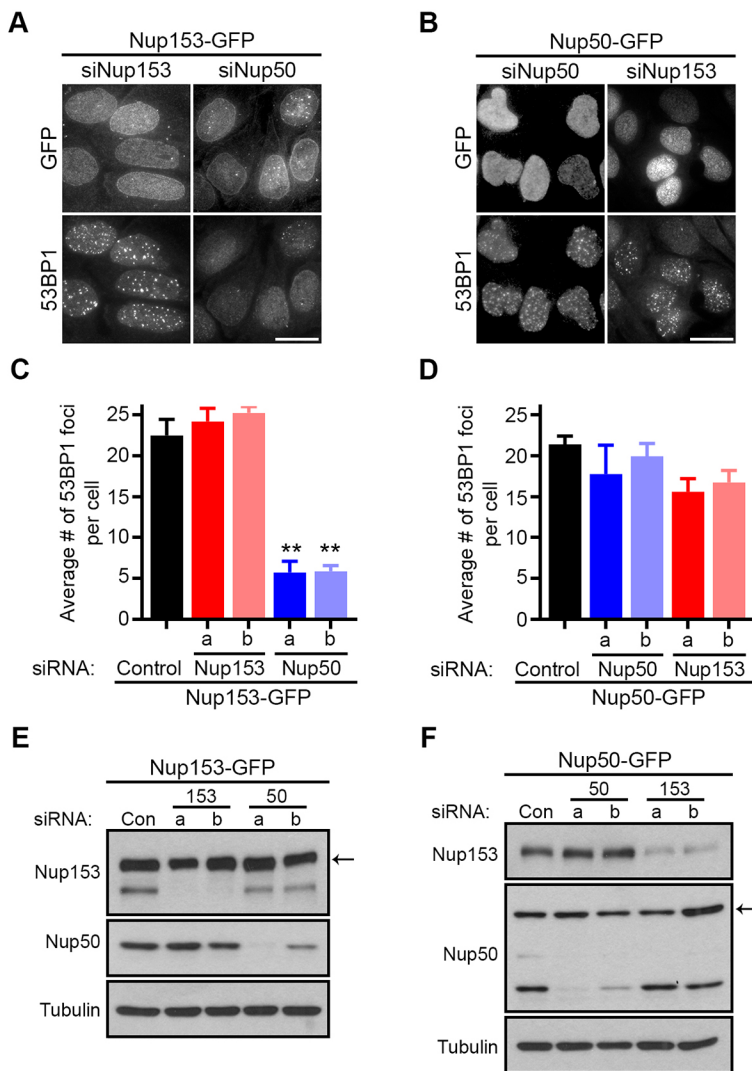


Fig. 5. Nup50-GFP expression is sufficient to rescue 53BP1 intranuclear targeting following Nup153 depletion. (A,B) U2OS cells stably expressing siRNA-resistant Nup153-GFP (A) or siRNA-resistant Nup50-GFP (B) were treated with the indicated siRNAs for 48 h, followed by a 30 min incubation in 20 μ M etoposide. Cells were fixed and analyzed using antibodies against GFP and 53BP1. Scale bars: 20 μ m. (C,D) Quantification of the average number of 53BP1 foci per nucleus as described previously. Error bars represent the mean and standard deviation from three independent experiments where >100 cells were scored. ** P <0.001 compared to control siRNA (Student's t -test). (E,F) Western blot analysis illustrating the efficiency of knockdown in each cell line. Arrow indicates Nup153-GFP and Nup50-GFP in E and F, respectively.

sufficient to override the requirement of Nup153 and Nup50 for 53BP1 localization. We found that BARD1-deficient cells displayed a phenotype that is strikingly similar to that of BRCA1-deficient cells – 53BP1 focal recruitment after treatment with either olaparib or etoposide was independent of Nup153 or Nup50 levels (Fig. 8; Fig. S3E). Together, our results point to the function of the BRCA1–BARD1 complex in preventing accumulation of 53BP1 at sites of DNA damage as the specific node in DNA damage response where Nup153 and Nup50 have a previously unappreciated counteracting role.

DISCUSSION

The results reported here provide novel insight into 53BP1 regulation during DNA damage response and are consistent with a model in which Nup153 and Nup50 normally promote 53BP1 targeting by opposing BRCA1-dependent events. Consequently, when levels of Nup153 or Nup50 are low, 53BP1 recruitment to double-strand breaks is impaired in a BRCA1-dependent manner. These observations further underscore the antagonism between BRCA1 and 53BP1 and, for the first time, place Nup153 and Nup50 in a molecular pathway that regulates this cross-talk. Integrating our results with previous reports defines at least three distinct steps at which Nup153 influences the response to DNA damage; in addition to previously reported roles in 53BP1 nuclear import (Moudry et al.,

2012) and in miRNA export (Wan et al., 2013), Nup153 promotes the intranuclear targeting of 53BP1 that is initiated immediately following DNA damage.

We also define for the first time the requirement for Nup50 in 53BP1 intranuclear targeting and demonstrate that loss of Nup50 binding impairs the role of Nup153 in this context. Indeed, Nup50 appears to be the critical nucleoporin with respect to delivery of 53BP1 to damage foci, as elevated levels of Nup50 rescue this activity in cells depleted of Nup153; overexpression of Nup153, in contrast, does not rescue this phenotype in Nup50-depleted cells. Cytoplasmic 53BP1 is still detected in Nup153-depleted cells that express elevated levels of Nup50, indicating that Nup50 does not play a role in 53BP1 import. Under these circumstances, nuclear concentrations of 53BP1 seem to be sufficient to restore focal recruitment – this was also the case in cells co-depleted of BRCA1 and Nup153, in which 53BP1 foci form in response to DNA damage despite persistence of the nuclear import defect. Consistent with a role for Nup50 specifically in intranuclear targeting of 53BP1, we noticed that Nup153 deletion variants that lack the ability to bind Nup50 retain the ability to rescue 53BP1 import, despite being impaired with respect to restoring 53BP1 recruitment to damage foci.

As many NPC proteins have been discovered to be multifunctional, understanding their different roles and determining

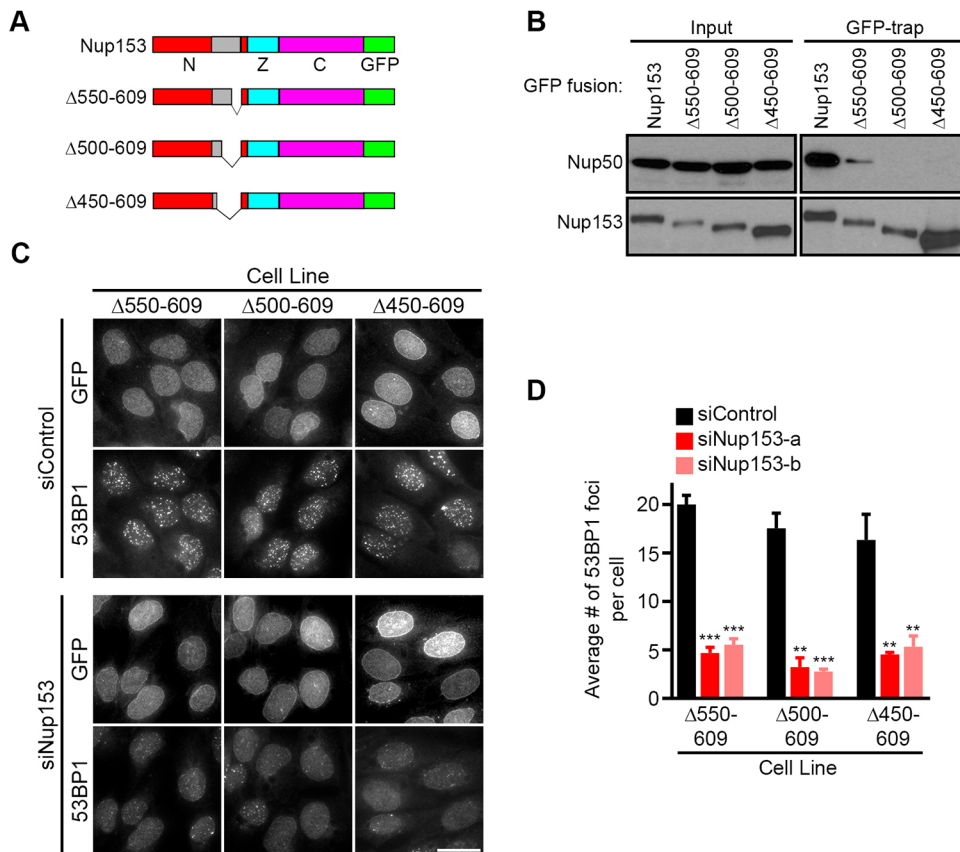


Fig. 6. Nup50 binding to Nup153 is required for 53BP1 intranuclear targeting. (A) First schematic: representation of the domain structure of Nup153, including the N (amino acids 1–658; red), Z (659–880; turquoise), and C (881–1475; magenta) domains. Also represented is the Nup50-binding domain (400–609; gray). Second to fourth schematics: Nup50 binding-deficient Nup153 variants ($\Delta 550-609$, $\Delta 500-609$, and $\Delta 450-609$) used in panels B–D. (B) GFP-fusion proteins were recovered from lysates that had been prepared from the indicated cell lines using the GFP-trap assay (see Materials and Methods). Recovery of Nup50 and GFP-fusion proteins was tracked by immunoblotting. (C) Cell lines stably expressing the indicated Nup153 variants were treated with the indicated siRNAs for 48 h, followed by a 30 min incubation in 20 μ M etoposide. Cells were then fixed and analyzed using antibodies against GFP and 53BP1. Scale bar: 20 μ m. (D) Quantification of the average number of 53BP1 foci per nucleus as described previously. Error bars represent the mean and standard deviation from three independent experiments where >100 cells were scored. ** $P < 0.001$, *** $P < 0.0001$; compared to control siRNA (Student's *t*-test).

whether these are distinct presents an experimental challenge. In this study, roles for Nup153 in the DNA damage response were uncoupled from each other. Complementing the information from depletion-rescue experiments discussed above, we found that a potent nuclear localization signal can rescue impaired import of 53BP1 following depletion of Nup153, but can not overcome the defect in targeting to damage foci. Furthermore, the rapid kinetics of this requirement for Nup153 make it unlikely to be due to its role in miRNA export (Wan et al., 2013) following DNA damage. Moreover, the role for Nup153 and Nup50 in 53BP1 intranuclear targeting is not attributable to previously discovered connections between these nucleoporins and the regulation of cytokinesis (Mackay et al., 2009, 2010) because (1) DNA damage response defects are prevalent in the cell population (>80%), whereas a delay at cytokinesis affects only 15–20% of cells in an otherwise asynchronous population and, (2) Nup50 depletion has only minor effects at the time of cytokinesis (Mackay et al., 2010), yet its depletion leads to equivalent defects in the DNA damage response compared to depletion of Nup153.

A common theme in recruitment of DNA damage response factors to sites of damage is the involvement of several layers of posttranslational modification, including phosphorylation, ubiquitylation and SUMOylation (Dantuma and van Attikum, 2016). In yeast, the NPC basket component Nup60 is required to maintain correct SUMOylation status of several DNA repair proteins through regulation of the Ulp1 SUMO protease (Palancade et al., 2007). As Nup153 is known to interact with the SUMO proteases SENP1 and SENP2 (Chow et al., 2012; Hang and Dasso, 2002; Zhang et al., 2002), modulation of SUMO status is clearly one way in which Nup153 could influence the DNA damage response. Consistent with this, a paper published while this manuscript was

in review reports a role for Nup153, in conjunction with SENP1, in promoting the SUMOylation of 53BP1 (Duheron et al., 2017). Notably, this function did not involve Nup50, suggesting that it relates to the Nup50-independent role Nup153 plays in promoting the robust import of 53BP1, or that the partnership between SENP1 and Nup153 contributes in yet another distinct manner to the DNA damage response.

Additionally, Nup153 and Nup50 are known to associate with chromatin (Ibarra et al., 2016; Jacinto et al., 2015; Kalverda et al., 2010) and – in the case of Nup153 – to promote certain chromatin modifications (Jacinto et al., 2015). While Nup153 and Nup50 do not accumulate at sites of DNA damage (Fig. S2), their distribution on the genome or their ability to transiently associate, may underlie a role in locally modulating the chromatin environment in response to DNA damage in a manner that allows 53BP1 binding. It also remains possible that Nup153 and Nup50 are required for nuclear import of an additional factor important for 53BP1 accumulation at damage sites. For instance, a recent study reported that mislocalization of Nup153 owing to aberrant expression of prelamin A results in defective nuclear import of 53BP1 through disruption of the Ran gradient (Cobb et al., 2016). However, our results, as well as those from Moudry et al., indicate that several well-characterized players in the DNA damage response, including γ -H2AX, MDC1, RNF8 and RNF168 are correctly recruited after Nup153 depletion (Moudry et al., 2012). Furthermore, depletion of Nup153 or Nup50 has little effect on general nuclear import or other aspects of NPC function (Buchwalter et al., 2014; Jacinto et al., 2015; Mackay et al., 2009, 2010).

An emerging model that may explain the mutual antagonism between 53BP1 and BRCA1 points toward the ubiquitylation of the nucleosomal subunit histone H2A as a node of regulation (Densham

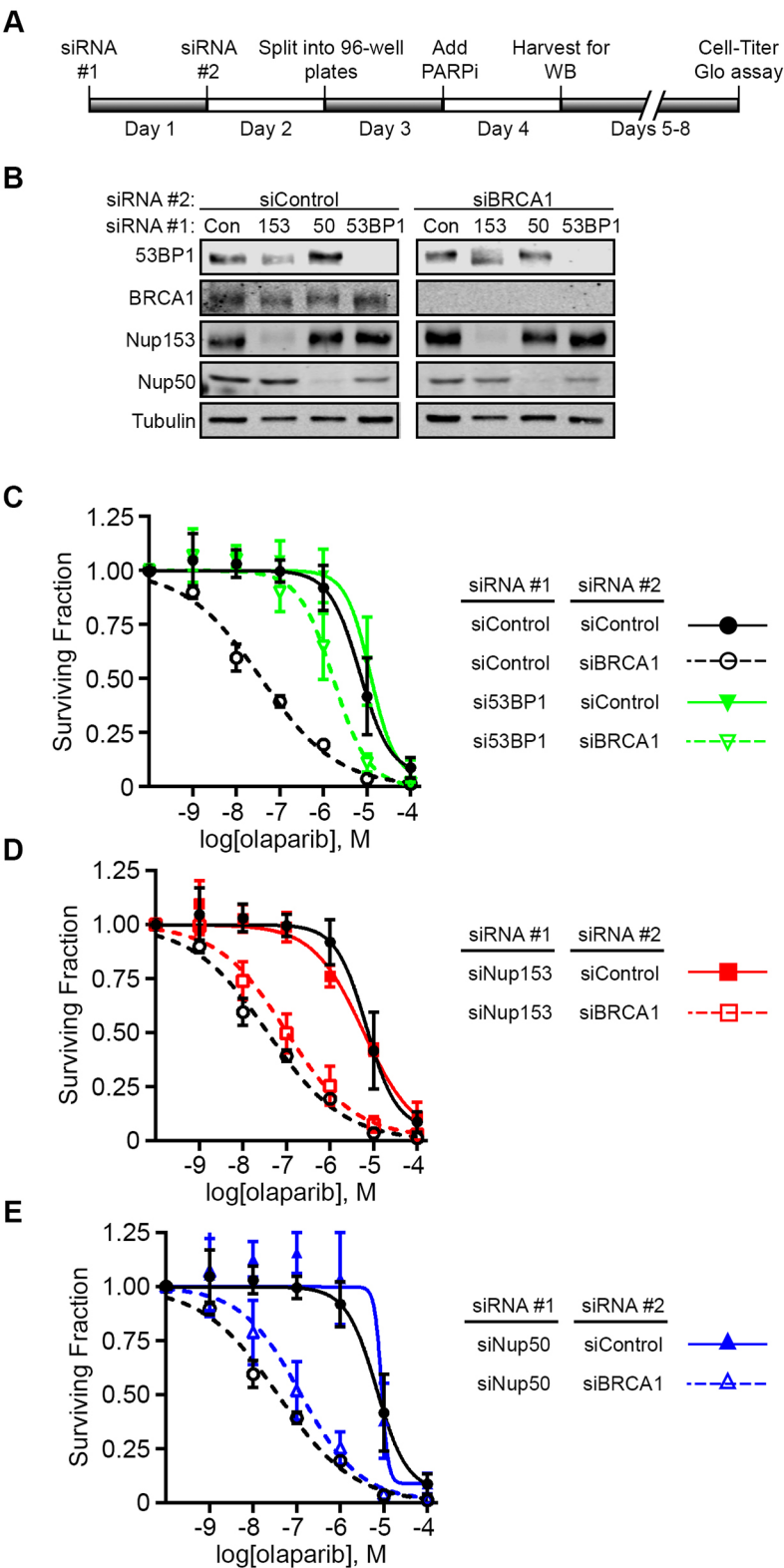


Fig. 7. 53BP1 depletion, but not Nup153 or Nup50 depletion, counteracts PARPi sensitivity in BRCA1-deficient cells. (A) Experimental timeline. Briefly, HeLa cells were treated first with either control or specific siRNA oligonucleotides to deplete 53BP1, Nup153 or Nup50 (siRNA #1), followed 24 h later by treatment with either control or BRCA1-specific siRNAs, as indicated (siRNA #2). The next day, $1-4 \times 10^3$ cells were seeded on 96-well assay plates and treated with increasing concentrations of olaparib for 5 days. At this point, cell viability was assessed using the Cell-Titer Glo assay. (B) Following both siRNA treatments, cells were incubated with 100 μ M olaparib and harvested 24 h later for western blot analysis. (C-E) Quantification of cell viability at the indicated olaparib concentrations. Control samples, with and without BRCA1 depletion, are shown in each graph for comparison. Error bars represent the mean and standard deviation of four independent experiments, and curves were fitted using GraphPad Prism.

et al., 2016). In response to DNA damage, ubiquitylation of histone H2A is catalyzed, in part, by the E3 ligase activity of BRCA1 in association with its requisite cofactor BARD1, leading to recruitment of the chromatin remodeler SMARCA1 (Densham et al., 2016; Kalb et al., 2014). Consequently, localized remodeling of the chromatin is thought to result in displacement of 53BP1 from the chromatin. Our observation that BARD1 depletion is sufficient

to override the requirement of Nup153 and Nup50 for 53BP1 targeting suggests that this regulatory mechanism is influenced by these nucleoporins, although other functions of BARD1, such as in maintaining BRCA1 stability (Fabbro et al., 2004), are not ruled out. Further studies are needed to integrate the roles of Nup153 and Nup50, and BRCA1–BARD1 in controlling recruitment of 53BP1 to repair foci.

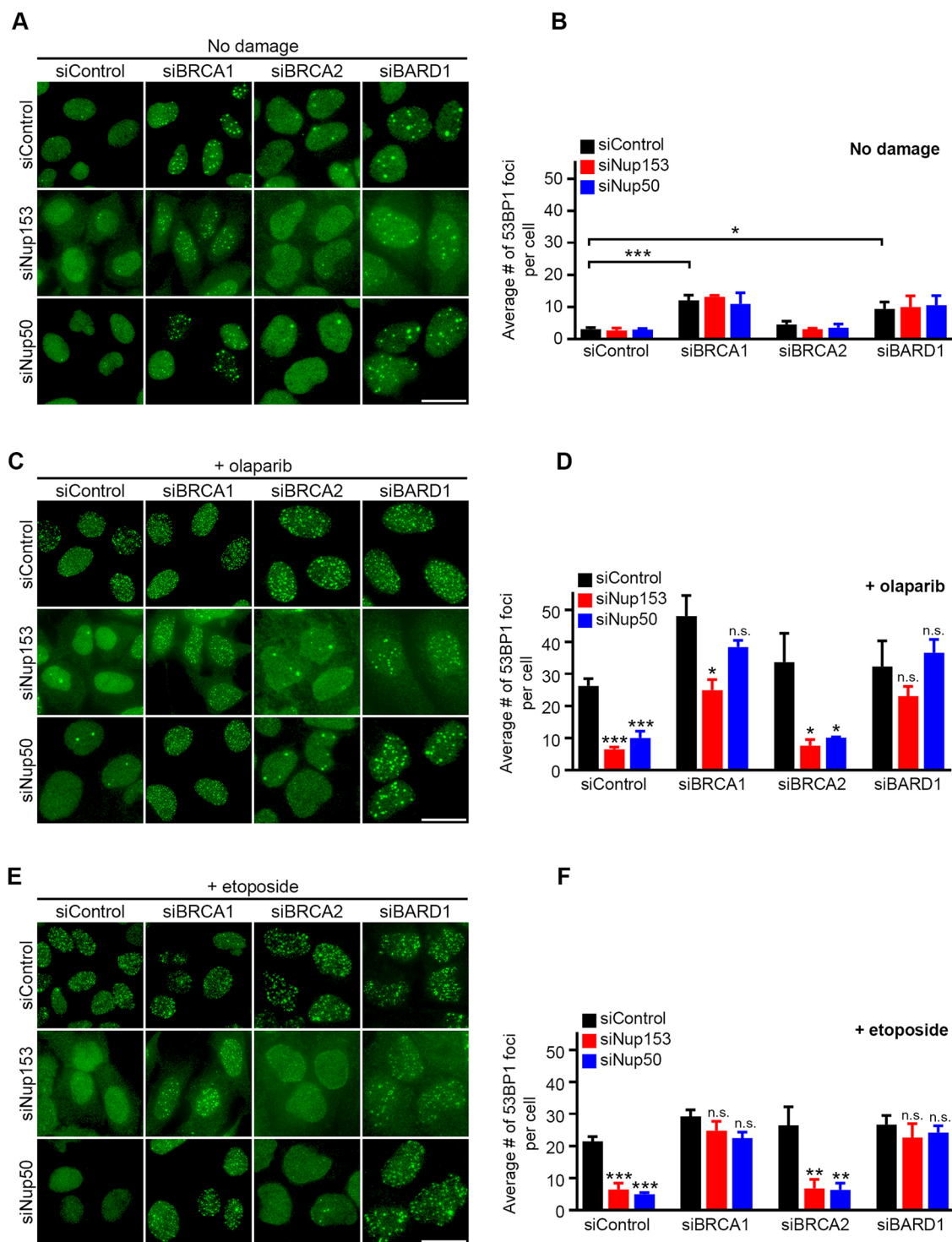


Fig. 8. 53BP1 focal targeting in response to PARPi or etoposide is insensitive to Nup153 or Nup50 levels when cells are deficient in BRCA1 or BARD1. (A,C,E) U2OS cells were treated according to the experimental timeline described for Fig. 7A, with the modification that cells were fixed and analyzed for the formation of 53BP1 foci (green) either 24 h after addition of DMSO (A; no damage) or 100 μ M olaparib (C), or 30 min after treatment with 20 μ M etoposide (E). Induction of DNA damage was confirmed by the presence of either MDC1-positive or γ -H2AX-positive foci (not shown). Scale bars: 20 μ m. (B,D,F) Quantification of the average number of 53BP1 foci per cell upon addition of DMSO (B), olaparib (D) or etoposide (F) after treatment with the indicated siRNA oligonucleotides. Error bars represent the mean and standard deviation from three independent experiments where >100 cells were scored. * P <0.01, ** P <0.005, *** P <0.001; n.s., not significant; compared to control siRNA within each group (black bars), except in B, where siControl-siControl treatment is compared with siControl-siBRCA1 or siControl-siBARD1 treatment (Student's t -test).

In addition to sparking new mechanistic questions, the results presented here can be considered in a clinical context as well. 53BP1 is actively being explored as a biomarker to help predict whether

BRCA1- or BRCA2-deficient tumors will respond to PARPi treatment (Pennington et al., 2013). Low or absent 53BP1 levels, or downstream effectors of 53BP1 such as REV7 and RIF1, are

associated with poor response or resistance to PARPi in both preclinical and *in vitro* models, underscoring the reliance of this treatment on a robust NHEJ repair pathway (Chapman et al., 2013; Escribano-Diaz et al., 2013; Jaspers et al., 2013; Xu et al., 2015; Zimmermann and de Lange, 2014). All of these models use BRCA1 deficiency as the experimental paradigm. Our results clarify that, while 53BP1 is important in this setting, levels of Nup153 and Nup50 are not critical to the response to PARPi in BRCA1-deficient cells. When we tested the requirement for 53BP1 in cellular toxicity following PARPi treatment of BRCA2-deficient cells, surprisingly, olaparib sensitivity did not necessarily require 53BP1 (Fig. S3). This challenge to the simple paradigm that PARPi toxicity always relies on NHEJ may be explained by other activities that have been ascribed to PARP enzymes (Gibson and Kraus, 2012; Gibson et al., 2016) or a route of NHEJ that does not rely on 53BP1. Nonetheless, it suggests that Nup153 and Nup50 – like 53BP1 – are not prime determinants of the response to PARPi in BRCA2-deficient tumors. The clinical scope of PARPi therapy is widening. PARPi is emerging as an effective treatment for not only a subset of breast and ovarian tumors but also (among others) prostate, pancreas and hematologic cancers, where defects in HR repair – not necessarily attributed to BRCA1 or BRCA2 deficiency – render them sensitive (Mateo et al., 2015; Ricks et al., 2015; Weston et al., 2010; Williamson et al., 2012). HR repair activity can also be disrupted pharmacologically by targeting signaling molecules such as ATM and ATR (Huehls et al., 2012; Konstantinopoulos et al., 2015; McCabe et al., 2006). Levels of Nup153 and Nup50 might be relevant in such settings if a robust 53BP1 response is required to mediate PARPi toxicity. Levels of Nup153 and Nup50 might also influence tumor response to other long-standing therapeutic strategies in oncology, such as treatment with cisplatin or even etoposide, both of which work by inducing DNA damage. The results reported here contribute to efforts to have a biomarker analysis that incorporates knowledge of pathway circuitry in order to predict therapeutic response with precision.

MATERIALS AND METHODS

Cell culture

U2OS and HeLa cells (not recently authenticated or tested for contamination) were grown in Dulbecco's modified Eagle's medium (Thermo Fisher, Carlsbad, CA) supplemented with 10% FBS at 37°C, 5% CO₂. DNA damage was induced by incubation with 20 µM etoposide (Selleck Chemicals, Houston, TX) for 30–120 min, as indicated in figure legends. In Figs 7 and 8, DNA damage was induced by treatment with 100 µM olaparib (ApexBio, Houston, TX) for 24 h. Where indicated, mirin (Millipore, Temecula, CA) was used at a concentration of 30 µM for 16 h before induction of DNA damage.

Transfection of siRNA

siRNA transfections were performed using Lipofectamine RNAiMAX (Thermo Fisher) according to manufacturer's instructions. siRNA sequences used are as follows: siControl (Mackay et al., 2009); siNup153-a (153-2) (Mackay et al., 2009); siNup153-b (153-1) (Mackay et al., 2009); siNup50-a (Ogawa et al., 2010); siNup50-b (J-012369-11-0005): 5'-GAAUAAUUGUGGACGGUACtt-3' (Thermo Fisher); siTpr-a (Mackay et al., 2010); siTpr-b (HS_TPR_4): 5'-GGGUGAAGAUAGUAUGAAtt-3' (Qiagen, Valencia, CA); si53BP1: 5'-GAAGGACGGAGUACUAAUAtt-3' (Tang et al., 2013); siBRCA1: 5'-AGAUAGUUCU-ACCAGUAAAtt-3' (Tang et al., 2013); siBRCA2: 5'-GGAUUUAUACA-UUUUCGCAtt-3' (Moudry et al., 2016); siBARD1: 5'-UGGUUUAG-CCCUCGAAGUAAGtt-3' (Densham et al., 2016). The 'a' set of oligonucleotides was used in the illustrations in all figures except for Fig. S1, where the 'b' set was used to confirm target specificity.

Plasmids and stable cell lines

GFP-53BP1 was constructed using the mCherry-53BP1 plasmid (Dimitrova et al., 2008) (Addgene, Cambridge, MA) by replacing mCherry with GFP

from the EGFP-N1 plasmid (Clontech, Mountain View, CA). GFP-53BP1-NLS was generated by adding a strong canonical NLS sequence (5'-PKKKRKV-3') in-frame at the 3'-end of GFP-53BP1 using PCR. Nup153^{Δ450-609}-GFP was generated by PCR using the Nup153-GFP plasmid as template. Cell lines stably expressing GFP-53BP1, GFP-53BP1-NLS, Nup153-GFP (Mackay et al., 2009), Nup50-GFP (Makise et al., 2012) and the Nup50-binding deficient variants of Nup153 were generated by transfecting the respective plasmids into U2OS cells using Lipofectamine LTX (Thermo Fisher) or Lipofectamine 3000 (Thermo Fisher) and selecting with 500 µg/ml G418.

Immunofluorescence, immunoblots and antibodies

Immunofluorescence

In general, cells were fixed for immunofluorescence analysis by either incubation in –20°C methanol for 10 min or 4% paraformaldehyde/PBS for 20 min at room temperature (RT), followed by incubation in PBS+0.5% Triton X-100. Antibody incubations were at RT for 2 h or at 4°C overnight in blocking solution (3% FBS+0.05% Triton in PBS). The following antibodies were used: 53BP1 (sc-22760; Santa Cruz Biotechnology, Dallas, TX; 1:1000); 53BP1 (MAB3802, Millipore; 1:2000); MDC1 (P2B11; Millipore; 1:500); γ-H2AX (JBW301; Millipore; 1:500); RIF1 (A300-569A; Bethyl Laboratories, Montgomery, TX; 1:500); Rad51 (ab133534; Abcam, Cambridge, MA; 1:1000); GFP (ab290; Abcam; 1:2000); Nup153 (SA1, provided by Brian Burke, Institute of Medical Biology, Singapore; 1:100); Nup50 (Mackay et al., 2010) (1:100); cyclin A (sc-271682; Santa Cruz Biotechnology; 1:1000). Secondary antibodies were purchased from Thermo Fisher. Coverslips were mounted in Fluoromount-G+DAPI (Southern Biotech, Birmingham, AL). Images were acquired with a Zeiss Axioskop2 microscope equipped with a 63× PlanApo (N.A. 1.4) objective. Fluorescence intensity measurements and 53BP1 foci quantification were performed using ImageJ (National Institutes of Health, Bethesda, MD). Briefly, nuclei were identified in the DAPI channel and manually selected as a region of interest. The 'Find Maxima' function in ImageJ was then used on each region of interest in the 53BP1 channel to count the number of foci.

Immunoblots

Samples for western blot were lysed in NP-40 lysis buffer [50 mM Tris-HCl (pH 8.0), 150 mM NaCl, 5 mM EDTA, 15 mM MgCl₂, 1% Nonidet P-40, 60 mM β-glycerophosphate, 1 mM DTT, 0.1 mM sodium vanadate, 100 µM PMSF and 0.1 Mm NaF, 1× Complete Protease Inhibitor Cocktail (Roche, Indianapolis, IN)]. Cleared lysates were then separated by SDS-PAGE, and transferred to PVDF membrane. Membranes were blocked in LI-COR blocking buffer and probed with primary antibodies according to manufacturer's instructions (LI-COR, Lincoln, NE). The following antibodies were used (if different from above): Tpr (IHC-00099; Bethyl Laboratories; 1:2000); BRCA1 (sc-6954; Santa Cruz Biotechnology; 1:200); BRCA2 (OP95; Millipore; 1:500); α-tubulin (YL1/2; Accurate Chemical & Scientific Corp., Westbury, NY; 1:2000); BARD1 (A300-263A; Bethyl Laboratories; 1:1000). Following incubation with LI-COR secondary antibodies, protein levels were detected using an Odyssey scanner (LI-COR). Alternatively, select immunoblots were instead probed with HRP-conjugated secondary antibodies (Thermo Fisher), incubated with Western Lightning Plus ECL reagent (Perkin Elmer, Waltham, MA), and exposed to film.

GFP-trap assay

Cell lysates prepared from cells expressing the indicated GFP-fusion proteins were prepared as described above. 500 µg of cell lysate was incubated with 10 µl of GFP-trap A beads (Chromotek) for 30 min at 4°C with rotation. Beads were then washed and bound proteins eluted with 2×SDS-PAGE loading dye.

Cell viability assay

HeLa cells were treated first with either control or specific siRNA oligonucleotides to deplete 53BP1, Nup153 or Nup50 (siRNA #1), followed 24 h later by treatment with either control or BRCA1-specific siRNAs, as indicated (siRNA #2). 48 h after the first siRNA transfection, 1–4×10³ cells were seeded on 96-well assay plates and treated 24 h later

with increasing concentrations of olaparib (1 nM–100 μ M) for 5 days. Cell viability was assessed using the Cell-Titer Glo assay (Promega, Madison, WI) according to manufacturer's instructions. The surviving fraction was calculated by comparing the luminescence at each olaparib concentration to that of samples without olaparib. Best-fit curves were generated using GraphPad Prism 6 (GraphPad Prism Software, La Jolla, CA).

Acknowledgements

We thank Trudy Oliver and Srividya Bhaskara for helpful comments and Masaki Makise and Jameika Price for technical assistance.

Competing interests

The authors declare no competing or financial interests.

Author contributions

Conceptualization: D.R.M., T.L.W., K.S.U.; Methodology: D.R.M.; Formal analysis: D.R.M., K.S.U.; Investigation: D.R.M., A.C.H.; Writing - original draft: D.R.M., K.S.U.; Writing - review & editing: D.R.M., T.L.W., K.S.U.; Supervision: D.R.M.; Project administration: K.S.U.; Funding acquisition: K.S.U.

Funding

This work was supported by the Progeria Research Foundation (#PRF-2013-48), the Huntsman Cancer Foundation, and the Women's Cancer Disease Oriented Team at the Huntsman Cancer Institute.

Supplementary information

Supplementary information available online at <http://jcs.biologists.org/lookup/doi/10.1242/jcs.203513.supplemental>

References

- Benarif, S. and Hall, M. (2015). An update on PARP inhibitors for the treatment of cancer. *Onco. Targets Ther.* **8**, 519–528.
- Bryant, H. E., Schultz, N., Thomas, H. D., Parker, K. M., Flower, D., Lopez, E., Kyle, S., Meuth, M., Curtin, N. J. and Helleday, T. (2005). Specific killing of BRCA2-deficient tumours with inhibitors of poly(ADP-ribose) polymerase. *Nature* **434**, 913–917.
- Buchwalter, A. L., Liang, Y. and Hetzer, M. W. (2014). Nup50 is required for cell differentiation and exhibits transcription-dependent dynamics. *Mol. Biol. Cell* **25**, 2472–2484.
- Bunting, S. F., Callén, E., Wong, N., Chen, H.-T., Polato, F., Gunn, A., Bothmer, A., Feldhahn, N., Fernandez-Capetillo, O., Cao, L. et al. (2010). 53BP1 inhibits homologous recombination in Brca1-deficient cells by blocking resection of DNA breaks. *Cell* **141**, 243–254.
- Cao, L., Xu, X., Bunting, S. F., Liu, J., Wang, R.-H., Cao, L. L., Wu, J. J., Peng, T.-N., Chen, J., Nussenzweig, A. et al. (2009). A selective requirement for 53BP1 in the biological response to genomic instability induced by Brca1 deficiency. *Mol. Cell* **35**, 534–541.
- Chapman, J. R., Sossick, A. J., Boulton, S. J. and Jackson, S. P. (2012). BRCA1-associated exclusion of 53BP1 from DNA damage sites underlies temporal control of DNA repair. *J. Cell Sci.* **125**, 3529–3534.
- Chapman, J. R., Barral, P., Vannier, J.-B., Borel, V., Steger, M., Tomas-Loba, A., Sartori, A. A., Adams, I. R., Batista, F. D. and Boulton, S. J. (2013). RIF1 is essential for 53BP1-dependent nonhomologous end joining and suppression of DNA double-strand break resection. *Mol. Cell* **49**, 858–871.
- Chow, K.-H., Elgort, S., Dasso, M. and Ullman, K. S. (2012). Two distinct sites in Nup153 mediate interaction with the SUMO proteases SENP1 and SENP2. *Nucleus* **3**, 349–358.
- Cobb, A. M., Larrieu, D., Warren, D. T., Liu, Y., Srivastava, S., Smith, A. J., Bowater, R. P., Jackson, S. P. and Shanahan, C. M. (2016). Prelamin A impairs 53BP1 nuclear entry by mislocalizing NUP153 and disrupting the Ran gradient. *Aging Cell* **15**, 1039–1050.
- Daigle, N., Beaudouin, J., Hartnell, L., Imreh, G., Hallberg, E., Lippincott-Schwartz, J. and Ellenberg, J. (2001). Nuclear pore complexes form immobile networks and have a very low turnover in live mammalian cells. *J. Cell Biol.* **154**, 71–84.
- Daley, J. M. and Sung, P. (2014). 53BP1, BRCA1, and the choice between recombination and end joining at DNA double-strand breaks. *Mol. Cell Biol.* **34**, 1380–1388.
- Dantuma, N. P. and van Attikum, H. (2016). Spatiotemporal regulation of posttranslational modifications in the DNA damage response. *EMBO J.* **35**, 6–23.
- Densham, R. M. and Morris, J. R. (2017). The BRCA1 Ubiquitin ligase function sets a new trend for remodelling in DNA repair. *Nucleus* **8**, 116–125.
- Densham, R. M., Garvin, A. J., Stone, H. R., Strachan, J., Baldock, R. A., Daza-Martin, M., Fletcher, A., Blair-Reid, S., Beesley, J., Johal, B. et al. (2016). Human BRCA1-BARD1 ubiquitin ligase activity counteracts chromatin barriers to DNA resection. *Nat. Struct. Mol. Biol.* **23**, 647–655.
- Di Virgilio, M., Callen, E., Yamane, A., Zhang, W., Jankovic, M., Gitlin, A. D., Feldhahn, N., Resch, W., Oliveira, T. Y., Chait, B. T. et al. (2013). RIF1 prevents resection of DNA breaks and promotes immunoglobulin class switching. *Science* **339**, 711–715.
- Dimitrova, N., Chen, Y.-C. M., Spector, D. L. and de Lange, T. (2008). 53BP1 promotes non-homologous end joining of telomeres by increasing chromatin mobility. *Nature* **456**, 524–528.
- Duheron, V., Chatel, G., Sauder, U., Oliveri, V. and Fahrenkrog, B. (2014). Structural characterization of altered nucleoporin Nup153 expression in human cells by thin-section electron microscopy. *Nucleus* **5**, 601–612.
- Duheron, V., Nilles, N., Pecenko, S., Martinelli, V. and Fahrenkrog, B. (2017). Localisation of Nup153 and SENP1 to nuclear pore complexes is required for 53BP1 mediated DNA double-strand break repair. *J. Cell Sci.* **130**, 2306–2316.
- Dultz, E., Zanin, E., Wurzenberger, C., Braun, M., Rabut, G., Sironi, L. and Ellenberg, J. (2008). Systematic kinetic analysis of mitotic dis- and reassembly of the nuclear pore in living cells. *J. Cell Biol.* **180**, 857–865.
- Dupré, A., Boyer-Chatenet, L., Sattler, R. M., Modi, A. P., Lee, J.-H., Nicolette, M. L., Kopelovich, L., Jasin, M., Baer, R., Paull, T. T. et al. (2008). A forward chemical genetic screen reveals an inhibitor of the Mre11-Rad50-Nbs1 complex. *Nat. Chem. Biol.* **4**, 119–125.
- Escobedo-Díaz, C., Orthwein, A., Fradet-Turcotte, A., Xing, M., Young, J. T., Tkáč, J., Cook, M. A., Rosebrock, A. P., Munro, M., Canny, M. D. et al. (2013). A cell cycle-dependent regulatory circuit composed of 53BP1-RIF1 and BRCA1-CtIP controls DNA repair pathway choice. *Mol. Cell* **49**, 872–883.
- Fabbro, M., Savage, K., Hobson, K., Deans, A. J., Powell, S. N., McArthur, G. A. and Khanna, K. K. (2004). BRCA1-BARD1 complexes are required for p53Ser-15 phosphorylation and a G1/S arrest following ionizing radiation-induced DNA damage. *J. Biol. Chem.* **279**, 31251–31258.
- Farmer, H., McCabe, N., Lord, C. J., Tutt, A. N. J., Johnson, D. A., Richardson, T. B., Santaros, M., Dillon, K. J., Hickson, I., Knights, C. et al. (2005). Targeting the DNA repair defect in BRCA mutant cells as a therapeutic strategy. *Nature* **434**, 917–921.
- Gibson, B. A. and Kraus, W. L. (2012). New insights into the molecular and cellular functions of poly(ADP-ribose) and PARPs. *Nat. Rev. Mol. Cell Biol.* **13**, 411–424.
- Gibson, B. A., Zhang, Y., Jiang, H., Hussey, K. M., Shrimp, J. H., Lin, H., Schwede, F., Yu, Y. and Kraus, W. L. (2016). Chemical genetic discovery of PARP targets reveals a role for PARP-1 in transcription elongation. *Science* **353**, 45–50.
- Griffis, E. R., Craige, B., Dimaano, C., Ullman, K. S. and Powers, M. A. (2004). Distinct functional domains within nucleoporins Nup153 and Nup98 mediate transcription-dependent mobility. *Mol. Biol. Cell* **15**, 1991–2002.
- Hang, J. and Dasso, M. (2002). Association of the human SUMO-1 protease SENP2 with the nuclear pore. *J. Biol. Chem.* **277**, 19961–19966.
- Hase, M. E. and Cordes, V. C. (2003). Direct interaction with nup153 mediates binding of Tpr to the periphery of the nuclear pore complex. *Mol. Biol. Cell* **14**, 1923–1940.
- Horigome, C., Bustard, D. E., Marcomini, I., Delgosaie, N., Tsai-Pflugfelder, M., Cobb, J. A. and Gasser, S. M. (2016). PolySUMOylation by Siz2 and Mms21 triggers relocation of DNA breaks to nuclear pores through the Slx5/Slx8 STUBL. *Genes Dev.* **30**, 931–945.
- Huehls, A. M., Wagner, J. M., Huntoon, C. J. and Karnitz, L. M. (2012). Identification of DNA repair pathways that affect the survival of ovarian cancer cells treated with a poly(ADP-ribose) polymerase inhibitor in a novel drug combination. *Mol. Pharmacol.* **82**, 767–776.
- Ibarra, A., Benner, C., Tyagi, S., Cool, J. and Hetzer, M. W. (2016). Nucleoporin-mediated regulation of cell identity genes. *Genes Dev.* **30**, 2253–2258.
- Jacinto, F. V., Benner, C. and Hetzer, M. W. (2015). The nucleoporin Nup153 regulates embryonic stem cell pluripotency through gene silencing. *Genes Dev.* **29**, 1224–1238.
- Jaspers, J. E., Kersbergen, A., Boon, U., Sol, W., van Deemter, L., Zander, S. A., Drost, R., Wientjens, E., Ji, J., Aly, A. et al. (2013). Loss of 53BP1 causes PARP inhibitor resistance in Brca1-mutated mouse mammary tumors. *Cancer Discov.* **3**, 68–81.
- Kakarougkas, A., Ismail, A., Klement, K., Goodarzi, A. A., Conrad, S., Freire, R., Shibata, A., Lobrich, M. and Jeggo, P. A. (2013). Opposing roles for 53BP1 during homologous recombination. *Nucleic Acids Res.* **41**, 9719–9731.
- Kalb, R., Mallory, D. L., Larkin, C., Huang, J. T. J. and Hiom, K. (2014). BRCA1 is a histone-H2A-specific ubiquitin ligase. *Cell Rep.* **8**, 999–1005.
- Kalouisi, A. and Soutoglou, E. (2016). Nuclear compartmentalization of DNA repair. *Curr. Opin. Genet. Dev.* **37**, 148–157.
- Kalverda, B., Pickersgill, H., Shloma, V. V. and Fornerod, M. (2010). Nucleoporins directly stimulate expression of developmental and cell-cycle genes inside the nucleoplasm. *Cell* **140**, 360–371.
- Knockenauer, K. E. and Schwartz, T. U. (2016). The nuclear pore complex as a flexible and dynamic gate. *Cell* **164**, 1162–1171.
- Konstantinopoulos, P. A., Ceccaldi, R., Shapiro, G. I. and D'Andrea, A. D. (2015). Homologous recombination deficiency: exploiting the fundamental vulnerability of ovarian cancer. *Cancer Discov.* **5**, 1137–1154.
- Lemaitre, C., Fischer, B., Kalouisi, A., Hoffbeck, A. S., Guirouilh-Barbat, J., Shahar, O. D., Genet, D., Goldberg, M., Bertrand, P., Lopez, B. et al. (2012). The

- nucleoporin 153, a novel factor in double-strand break repair and DNA damage response. *Oncogene* **31**, 4803–4809.
- Liu, J. F., Konstantinopoulos, P. A. and Matulonis, U. A. (2014). PARP inhibitors in ovarian cancer: current status and future promise. *Gynecol. Oncol.* **133**, 362–369.
- Lord, C. J. and Ashworth, A. (2013). Mechanisms of resistance to therapies targeting BRCA-mutant cancers. *Nat. Med.* **19**, 1381–1388.
- Mackay, D. R., Elgort, S. W. and Ullman, K. S. (2009). The nucleoporin Nup153 has separable roles in both early mitotic progression and the resolution of mitosis. *Mol. Biol. Cell* **20**, 1652–1660.
- Mackay, D. R., Makise, M. and Ullman, K. S. (2010). Defects in nuclear pore assembly lead to activation of an Aurora B-mediated abscission checkpoint. *J. Cell Biol.* **191**, 923–931.
- Makise, M., Mackay, D. R., Elgort, S., Shankaran, S. S., Adam, S. A. and Ullman, K. S. (2012). The Nup153-Nup50 protein interface and its role in nuclear import. *J. Biol. Chem.* **287**, 38515–38522.
- Mateo, J., Carreira, S., Sandhu, S., Miranda, S., Mossop, H., Perez-Lopez, R., Nava Rodrigues, D., Robinson, D., Omlin, A., Tunariu, N. et al. (2015). DNA-repair defects and olaparib in metastatic prostate cancer. *N. Engl. J. Med.* **373**, 1697–1708.
- McCabe, N., Turner, N. C., Lord, C. J., Kluzek, K., Bialkowska, A., Swift, S., Giavara, S., O'Connor, M. J., Tutt, A. N., Zdzienicka, M. Z. et al. (2006). Deficiency in the repair of DNA damage by homologous recombination and sensitivity to poly(ADP-ribose) polymerase inhibition. *Cancer Res.* **66**, 8109–8115.
- Moudry, P., Lukas, C., Macurek, L., Neumann, B., Heriche, J.-K., Pepperkok, R., Ellenberg, J., Hodny, Z., Lukas, J. and Bartek, J. (2012). Nucleoporin NUP153 guards genome integrity by promoting nuclear import of 53BP1. *Cell Death Differ.* **19**, 798–807.
- Moudry, P., Watanabe, K., Wolanin, K. M., Bartkova, J., Wassing, I. E., Watanabe, S., Strauss, R., Troelsgaard Pedersen, R., Oestergaard, V. H., Lisby, M. et al. (2016). TOPBP1 regulates RAD51 phosphorylation and chromatin loading and determines PARP inhibitor sensitivity. *J. Cell Biol.* **212**, 281–288.
- Moynahan, M. E., Pierce, A. J. and Jasin, M. (2001). BRCA2 is required for homology-directed repair of chromosomal breaks. *Mol. Cell* **7**, 263–272.
- Nagai, S., Dubrana, K., Tsai-Pflugfelder, M., Davidson, M. B., Roberts, T. M., Brown, G. W., Varela, E., Hediger, F., Gasser, S. M. and Krogan, N. J. (2008). Functional targeting of DNA damage to a nuclear pore-associated SUMO-dependent ubiquitin ligase. *Science* **322**, 597–602.
- Ogawa, Y., Miyamoto, Y., Asally, M., Oka, M., Yasuda, Y. and Yoneda, Y. (2010). Two isoforms of Np60 (Nup50) differentially regulate nuclear protein import. *Mol. Biol. Cell* **21**, 630–638.
- Oplustilova, L., Wolanin, K., Mistrik, M., Korinkova, G., Simkova, D., Bouchal, J., Lenobel, R., Bartkova, J., Lau, A., O'Connor, M. J. et al. (2012). Evaluation of candidate biomarkers to predict cancer cell sensitivity or resistance to PARP-1 inhibitor treatment. *Cell Cycle* **11**, 3837–3850.
- Oza, P., Jaspersen, S. L., Miele, A., Dekker, J. and Peterson, C. L. (2009). Mechanisms that regulate localization of a DNA double-strand break to the nuclear periphery. *Genes Dev.* **23**, 912–927.
- Palancade, B., Liu, X., Garcia-Rubio, M., Aguilera, A., Zhao, X. and Doye, V. (2007). Nucleoporins prevent DNA damage accumulation by modulating Ulp1-dependent sumoylation processes. *Mol. Biol. Cell* **18**, 2912–2923.
- Patel, A. G., Sarkaria, J. N. and Kaufmann, S. H. (2011). Nonhomologous end joining drives poly(ADP-ribose) polymerase (PARP) inhibitor lethality in homologous recombination-deficient cells. *Proc. Natl. Acad. Sci. USA* **108**, 3406–3411.
- Pennington, K. P., Wickramanayake, A., Norquist, B. M., Pennil, C. C., Garcia, R. L., Agnew, K. J., Taniguchi, T., Welsh, P. and Swisher, E. M. (2013). 53BP1 expression in sporadic and inherited ovarian carcinoma: relationship to genetic status and clinical outcomes. *Gynecol. Oncol.* **128**, 493–499.
- Rabut, G., Doye, V. and Ellenberg, J. (2004). Mapping the dynamic organization of the nuclear pore complex inside single living cells. *Nat. Cell Biol.* **6**, 1114–1121.
- Ricks, T. K., Chiu, H.-J., Ison, G., Kim, G., McKee, A. E., Kluetz, P. and Pazdur, R. (2015). Successes and challenges of PARP inhibitors in cancer therapy. *Front Oncol.* **5**, 222.
- Rogakou, E. P., Pilch, D. R., Orr, A. H., Ivanova, V. S. and Bonner, W. M. (1998). DNA double-stranded breaks induce histone H2AX phosphorylation on serine 139. *J. Biol. Chem.* **273**, 5858–5868.
- Sandhu, S. K., Yap, T. A. and de Bono, J. S. (2010). Poly(ADP-ribose) polymerase inhibitors in cancer treatment: a clinical perspective. *Eur. J. Cancer* **46**, 9–20.
- Smith-Roe, S. L., Nakamura, J., Holley, D., Chastain, P. D., II, Rosson, G. B., Simpson, D. A., Ridpath, J. R., Kaufman, D. G., Kaufmann, W. K. and Bultman, S. J. (2015). SWI/SNF complexes are required for full activation of the DNA-damage response. *Oncotarget* **6**, 732–745.
- Tang, J., Cho, N. W., Cui, G., Manion, E. M., Shanbhag, N. M., Botuyan, M. V., Mer, G. and Greenberg, R. A. (2013). Acetylation limits 53BP1 association with damaged chromatin to promote homologous recombination. *Nat. Struct. Mol. Biol.* **20**, 317–325.
- Tutt, A., Bertwistle, D., Valentine, J., Gabriel, A., Swift, S., Ross, G., Griffin, C., Thacker, J. and Ashworth, A. (2001). Mutation in Brca2 stimulates error-prone homology-directed repair of DNA double-strand breaks occurring between repeated sequences. *EMBO J.* **20**, 4704–4716.
- Wan, G., Zhang, X., Langley, R. R., Liu, Y., Hu, X., Han, C., Peng, G., Ellis, L. M., Jones, S. N. and Lu, X. (2013). DNA-damage-induced nuclear export of precursor microRNAs is regulated by the ATM-AKT pathway. *Cell Rep.* **3**, 2100–2112.
- Weston, V. J., Oldreive, C. E., Skowronska, A., Oscier, D. G., Pratt, G., Dyer, M. J. S., Smith, G., Powell, J. E., Rudzki, Z., Kearns, P. et al. (2010). The PARP inhibitor olaparib induces significant killing of ATM-deficient lymphoid tumor cells in vitro and in vivo. *Blood* **116**, 4578–4587.
- Williamson, C. T., Kubota, E., Hamill, J. D., Klimowicz, A., Ye, R., Muzik, H., Dean, M., Tu, L. R., Gilley, D., Magliocco, A. M. et al. (2012). Enhanced cytotoxicity of PARP inhibition in mantle cell lymphoma harbouring mutations in both ATM and p53. *EMBO Mol. Med.* **4**, 515–527.
- Xu, G., Chapman, J. R., Brandsma, I., Yuan, J., Mistrik, M., Bouwman, P., Bartkova, J., Gogola, E., Warmerdam, D., Barazas, M. et al. (2015). REV7 counteracts DNA double-strand break resection and affects PARP inhibition. *Nature* **521**, 541–544.
- Yang, K. S., Kohler, R. H., Landon, M., Giedt, R. and Weissleder, R. (2015). Single cell resolution in vivo imaging of DNA damage following PARP inhibition. *Sci. Rep.* **5**, 10129.
- Zhang, H., Saitoh, H. and Matunis, M. J. (2002). Enzymes of the SUMO modification pathway localize to filaments of the nuclear pore complex. *Mol. Cell Biol.* **22**, 6498–6508.
- Zhang, H., Liu, H., Chen, Y., Yang, X., Wang, P., Liu, T., Deng, M., Qin, B., Correia, C., Lee, S. et al. (2016). A cell cycle-dependent BRCA1-UHRF1 cascade regulates DNA double-strand break repair pathway choice. *Nat. Commun.* **7**, 10201.
- Zimmermann, M. and de Lange, T. (2014). 53BP1: pro choice in DNA repair. *Trends Cell Biol.* **24**, 108–117.
- Zimmermann, M., Lottersberger, F., Buonomo, S. B., Sfeir, A. and de Lange, T. (2013). 53BP1 regulates DSB repair using Rif1 to control 5' end resection. *Science* **339**, 700–704.